Journal of Nuclear Science and Technology

ISSN: 0022-3131 (Print) 1881-1248 (Online) Journal homepage: www.tandfonline.com/journals/tnst20

Initial dissolution rate of a Japanese simulated high-level waste glass P0798 as a function of pH and temperature measured by using micro-channel flow-through test method

Yaohiro Inagaki, Hikaru Makigaki, Kazuya Idemitsu, Tatsumi Arima, Sei-Ichiro Mitsui & Kenji Noshita

To cite this article: Yaohiro Inagaki, Hikaru Makigaki, Kazuya Idemitsu, Tatsumi Arima, Sei-Ichiro Mitsui & Kenji Noshita (2012) Initial dissolution rate of a Japanese simulated high-level waste glass P0798 as a function of pH and temperature measured by using micro-channel flow-through test method, Journal of Nuclear Science and Technology, 49:4, 438-449, DOI: 10.1080/00223131.2012.669246

To link to this article: https://doi.org/10.1080/00223131.2012.669246

Published online: 28 Mar 2012.

Journal of Nuclear Science and Technology
Volume 49, No. 4, April (2012) pp. 438–449
http://www.tandfonline.com

Taylor & Francis
Taylor & Francis Group

ARTICLE

Initial dissolution rate of a Japanese simulated high-level waste glass P0798 as a function of pH and temperature measured by using micro-channel flow-through test method

Yaohiro Inagaki[a]*, Hikaru Makigaki[a], Kazuya Idemitsu[a], Tatsumi Arima[a], Sei-Ichiro Mitsui[b] and Kenji Noshita[c]

[a]*Department of Applied Quantum Physics & Nuclear Engineering, Kyushu University, Fukuoka 819-0395, Japan;* [b]*Geological Isolation Research and Development Directorate, Japan Atomic Energy Agency, Ibaraki 319-1194, Japan;* [c]*Hitachi Research Laboratory, Hitachi Ltd., Ibaraki 319-1221, Japan*

(*Received 2 September 2011; accepted final version for publication 26 December 2011*)

Aqueous dissolution tests were performed for a Japanese type of simulated high-level waste (HLW) glass P0798 by using a newly developed test method of micro-channel flow-through (MCFT) method, and the initial dissolution rate of glass matrix, r_0, was measured as a function of solution pH (3–11) and temperature (25–90°C) precisely and consistently for systematic evaluation of the dissolution kinetics. The MCFT method using a micro-channel reactor with a coupon shaped glass specimen has the following features to provide precise and consistent data on the glass dissolution rate: (1) any controlled constant solution condition can be provided over the test duration; (2) the glass surface area actually reacting with solution can be determined accurately; and (3) direct and totally quantitative analyses of the reacted glass surface can be performed for confirming consistency of the test results. The present test results indicated that the r_0 shows a ''V-shaped'' pH dependence with a minimum at around pH 6 at 25°C, but it changes to a ''U-shaped'' one with a flat bottom at neutral pH at elevated temperatures of up to 90°C. The present results also indicated that the r_0 increases with temperature according to an Arrhenius law at any pH, and the apparent activation energy evaluated from Arrhenius relation increases with pH from 54 kJ/mol at pH 3 to 76 kJ/mol at pH 10, which suggests that the dissolution mechanism changes depending on pH.

Keywords: HLW glass; dissolution kinetics; initial dissolution rate; micro-channel flow-through test method; pH dependence; temperature dependence; activation energy; dissolution mechanism

1. Introduction

Over the last few decades, understanding the processes of radioactive waste glass dissolution in aqueous media has advanced through a large number of the dissolution tests performed by many researchers in the world, and modeling the glass dissolution for long-term geological disposal has also advanced on the basis of the advanced understandings of dissolution processes. For assessing the long-term glass performance in geological disposal with assurance, however, we need a greater understanding of kinetics for the glass dissolution under the actual or potential repository conditions in consideration of the long-term evolution of the repository conditions. The greater understanding of the dissolution kinetics is also required for parameterization of a mechanistic model used to determine the rate of glass dissolution or radionuclide release as a function of key environmental variables such as the solution composition, pH, flow rate, temperature, reaction progress, and time.

In order to understand the glass dissolution kinetics further, we need precise and consistent experimental data on the glass dissolution rate measured systematically under various well-constrained test conditions. A very large number of dissolution tests have been performed for the waste glasses throughout the world; however, there have been only a few precise and consistent data available for systematic evaluation of the dissolution kinetics. With respect to pH dependence of the glass dissolution rate, for example, we have only a few reliable data sets measured precisely and consistently, because the test conditions such as the solution composition, pH, and the glass surface area can change easily during the test period against the expectations as a consequence of the nature of the current standard test methods such as MCC (Material Characterization Center) and PCT (Product Consistency Tests) test methods [1]. For the further

*Corresponding author. Email: inagakiyh@nucl.kyushu-u.ac.jp

ISSN 0022-3131 print/ISSN 1881-1248 online

http://dx.doi.org/10.1080/00223131.2012.669246

evaluation of the dissolution kinetics, therefore, we should improve or develop the test methods to measure the glass dissolution rate precisely and consistently under various well-constrained test conditions.

Several test methods have been developed and applied to measurement of the glass dissolution kinetics for the last few decades [1–3], and these test methods can be categorized into two types, i.e., "static method" and "flow-through method." Although both types have been applied to the measurement, the flow-through method is adequate for the measurement of the dissolution kinetics, e.g., measurement of the dissolution rate as a function of the key environmental variables, since the flow-through method can provide any controlled constant solution condition easily over the test duration. Single pass flow-through (SPFT) method is one of the major flow-through test methods of great use, and it has been applied to the measurement of the glass dissolution rate as a function of environmental variables [3–5]. In the SPFT method, the powdered glass specimen packed in a reaction cell is usually used in order to provide a high S/V (glass surface area to solution volume) ratio leading to a quick increase in solution concentrations of dissolved glass constituent elements for precise solution analysis. The use of powdered glass specimen, on the other hand, causes a difficulty in accurate determination of the glass surface area actually reacting with solution, because the actually reacting surface area sometimes differs from the surface area measured by using BET (Brunauer-Emmett-Teller) method for finely powdered glass specimen [6]. In addition, the progress of glass dissolution may cause a certain decrease in the glass surface area during the test period for powdered glass specimen. Since the glass dissolution rate is usually represented with a unit of $g/m^2/day$, an error in determination of the surface area causes directly an error in determination of the glass dissolution rate. The use of powdered glass specimen also causes a difficulty in direct analyses of the reacted glass surface to obtain the totally quantitative data, such as the glass dissolution depth from the initial surface and elemental distribution profile on/in the surface layer, though quantitative comparison between the solution analysis data and the reacted glass surface analysis data is required to confirm consistency of the test results. Consequently, the glass dissolution rate measured by using SPFT method may remain some uncertainties for further evaluation of the dissolution kinetics in an aspect of the preciseness and consistency.

Therefore, we have applied a newly developed flow-through test method using micro-channel reactor to precise and consistent measurement of the glass dissolution kinetics [7,8]. In this test method named "micro-channel flow-through (MCFT) method," a coupon shaped glass is used as a specimen, which allows accurate determination of the glass surface area actually reacting with solution. In spite of using the coupon shaped glass specimen, the use of micro-channel reactor can provide a relatively high S/V ratio to allow precise solution analysis, by which the glass dissolution rate can be determined precisely. In addition, the use of coupon shaped glass specimen enables direct analyses of the reacted glass surface to obtain the totally quantitative data on the reacted glass surface for confirming consistency of the test results.

In the present study, therefore, aqueous dissolution tests were performed by using MCFT method for a Japanese type of simulated high-level waste (HLW) glass P0798, and the initial dissolution rate of glass matrix, which is one of the intrinsic parameters for glass–water reactions, was measured as a function of solution pH and temperature precisely and consistently. On the basis of the precise and consistent data obtained systematically by the present test, the glass dissolution kinetics was discussed.

2. Experimental

2.1. Glass specimen

A Japanese type of simulated borosilicate waste glass P0798 fabricated by Japan Atomic Energy Agency (JAEA) was used as a specimen. The chemical composition of P0798 glass is shown in **Table 1**, which is close to that of French SON68 glass. The bulk glass was cut into a coupon shaped one (30 mm × 10 mm × 4 mm size), and the surface was conditioned by polishing with finally 1 μm DP (diamond paste) using alcohol lubricant to prevent selective dissolution of soluble elements such as Na, Li, and B during polishing.

2.2. The MCFT test method

Figure 1 shows schematics of the MCFT test apparatus. The test apparatus has been originally developed by Okuyama et al. in order to measure both diffusion and sorption coefficients of rock medium [9,10], and it has been modified to suit measurement of the glass dissolution/alteration kinetics by Inagaki et al. [7,8]. The test apparatus

Table 1. Chemical composition of P0798 simulated waste glass (wt%) [7].

SiO_2	46.60	Rb_2O	0.11	SeO_2	0.02
B_2O_3	14.20	Cs_2O	0.75	TeO_2	0.19
Al_2O_3	5.00	SrO	0.30	Y_2O_3	0.18
Li_2O	3.00	BaO	0.49	La_2O_3	0.42
CaO	3.00	ZrO_2	1.46	CeO_2	3.34
ZnO	3.00	MoO_3	1.45	Pr_6O_{11}	0.42
		MnO_2	0.37	Nd_2O_3	1.38
Na_2O	10.00	RuO_2	0.74	Sm_2O_3	0.29
P_2O_5	0.30	Rh_2O_3	0.14	Eu_2O_3	0.05
		PdO	0.35	Gd_2O_3	0.02
Fe_2O_3	2.04	Ag_2O	0.02	–	–
NiO	0.23	CdO	0.02	Total	100
Cr_2O_3	0.10	SnO_2	0.02		

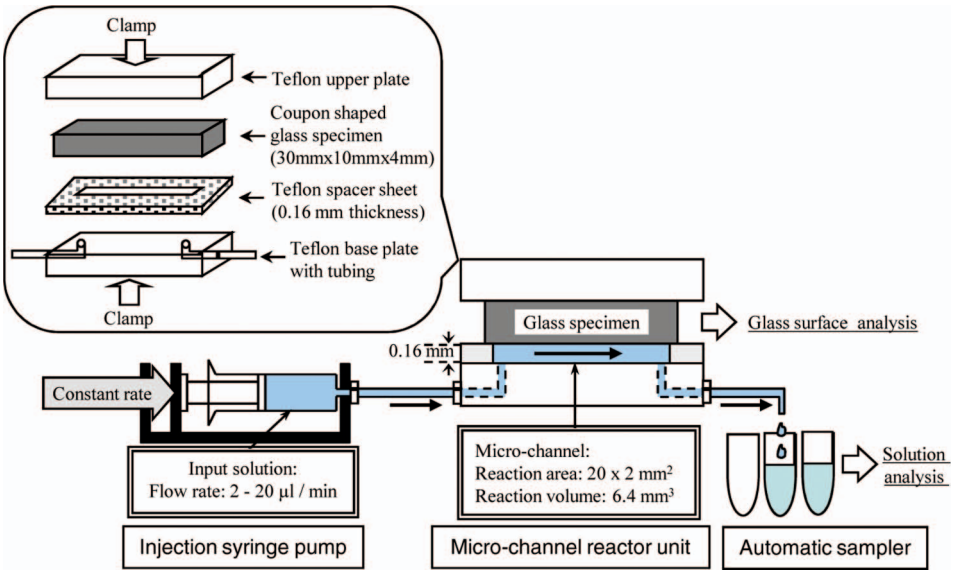

Figure 1. Schematics of the MCFT test apparatus.

consisted of three parts: an injection syringe pump, a micro-channel reactor unit, and an automatic sampler, being connected with each other with PTFE (polytetrafluoroethylene, Teflon®) tubing. In the micro-channel reactor unit, a face of coupon shaped glass specimen was in contact with a micro-channel (20 mm length, 2 mm width, 0.16 mm depth) constructed on a PTFE plate with a spacer sheet, and a solution was injected into the inlet of micro-channel at a constant rate with a syringe pump. The injected solution flew through the micro-channel reacting with the glass to the outlet, and the outlet solution was retrieved at certain intervals with an automatic sampler to be analyzed for the determination of the dissolution rate of each glass constituent element at each sampling. Consequently, the glass dissolution/alteration rate was determined as a function of reaction time by plotting the rate determined at each sampling continuously. After the test, the glass specimen removed from the micro-channel reactor was subjected to direct measurement of the glass dissolution depth from the initial surface for confirming consistency of the data on the dissolution rate determined from the solution analysis.

Features of the MCFT test method are summarized as follows: (1) any controlled constant solution condition, such as solution composition and pH, can be provided over the test duration; (2) the glass surface area actually reacting with solution can be determined accurately by using a coupon shaped glass specimen; (3) a relatively high S/V ratio for precise solution analysis can be provided by using micro-channel reactor; (4) direct and totally quantitative glass surface analyses can be performed by using a coupon shaped glass specimen for confirming consistency of the test results. These features can contribute to a precise and consistent measurement of the glass dissolution rate under various environmental conditions needed for the kinetic evaluation. The additional features are: (5) the glass dissolution/alteration rate can be determined directly at each short sampling period; and (6) the test apparatus is simple with compact size and easy operation, which allows a flexible setup of test conditions.

2.3. *Test procedure and conditions*

Aqueous dissolution tests using MCFT method were performed for P0798 glass as a function of solution pH (pH 3–11) and temperature (25–90°C) for test duration of up to 100 h with each sampling period of 2–5 h. The solution flow rate was selected to be 5 μl/min according to our previous studies [7,8] where the glass dissolution rate at 25°C has been confirmed to be independent of the solution flow rate in the range from 2 μl/min to 20 μl/min. The apparent S/V ratio was evaluated to be 6400 m^{-1} based on the dimensions of micro-channel (20 mm length, 2 mm width, 0.16 mm depth) shown in Figure 1 on the assumption that the inner volume of PTFE tube can be ignored. The inlet solution was 10^{-3} M KCl solution, and the pH was adjusted to be 3, 4, 5.6, 6.9, 8, 10, and 11, respectively, by addition of ultra-pure grade HCl or KOH solutions. Since the solution pH changes with temperature, the pH at each elevated temperature was estimated by using geochemical calculation code PHREEQE-C [11] on the assumption that total amount of dissolved CO_2 (ΣCO_2) at 25°C is conserved at each elevated temperature. Configuration of the test apparatus is shown in **Figure 2**. The tests were performed by placing the micro-channel reactor unit with PTFE tubing in an

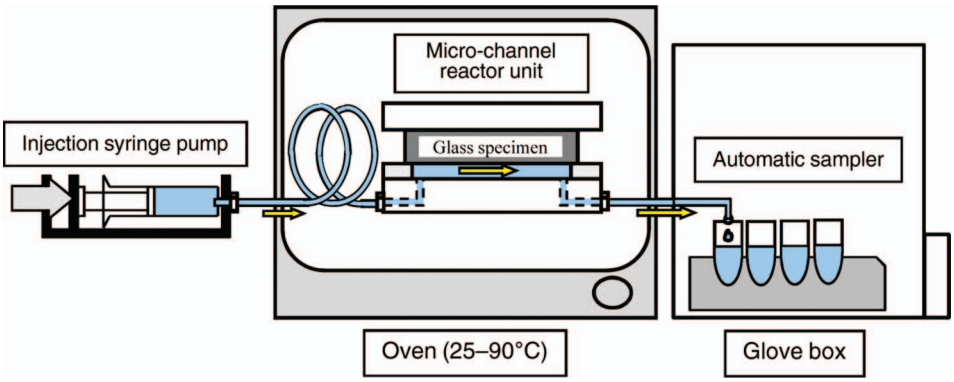

Figure 2. Configuration of MCFT test apparatus.

oven to maintain the temperature and by placing the automatic sampler in a glove box to prevent evaporation loss of sampling solution.

The concentrations of Si, B, and Cs in the output solution were measured at each sampling by using ICP-MS (Inductively Coupled Plasma Mass Spectrometry, model 7500c, Agilent Technologies, Inc.) after dilution with ultra-pure grade HNO_3 solution. After the test, the glass specimen removed from the micro-channel reactor was dried at room temperature for a few days to be subjected to the surface analyses where the glass dissolution depth from the original surface was directly measured by using a surface roughness analyzer (model Dektak 3ST, ULVAC, Inc.). **Table 2** summarizes the conditions and parameters examined in the present tests.

For evaluating the regime of solution flow in the micro-channel, the Reynolds number was calculated under the present test conditions (solution flow rate of 5–20 μl/min, and micro-channel dimensions of 20 mm length, 2mm width, 0.16 mm depth) to be less than 0.5, which indicates that the regime of solution flow was completely laminar flow.

Table 2. Summary of dissolution test conditions and parameters.

Test method	MCFT method Dimension of micro-channel: 20 mm × 2 mm × 0.16 mm
Glass	P0798 simulated HLW glass Size: 30 mm × 10 mm × 4 mm Surface condition: polished with 1 μm DP
Solution	10^{-3} M KCl solution pH 3–11 (adjusted by addition of HCl or KOH)
Temperature	25, 50, 70, 90°C
Solution flow rate	5 μl/min (0.3 ml/h) Optional case: 20 μl/min (1.2 ml/h)
S/V ratio	Apparently 6400 m^{-1}
Reaction time	Up to 100 h (partly up to 270 h)
Solution analysis	Concentrations of Si, B, and Cs in output solution measured by using ICP-MS
Glass surface analysis	Dissolution depth profile measured by using surface roughness analyzer

2.4. *Determination of dissolution rate*

The dissolution rate of element i from glass was determined at each sampling as normalized dissolution rate, NR_i, by using the following equation:

$$NR_i[\mathrm{g/m^2/day}] = \frac{C_i}{\Delta t}\frac{1}{f_i}\frac{V}{S} \quad (1)$$

where NR_i is the normalized dissolution rate of element i at each sampling; C_i is the concentration of element i in output solution at each sampling; Δt represents each sampling period; f_i is the mass fraction of element i in original glass; V is the output solution volume at each sampling; and S is the geometric glass surface area in contact with solution.

Consequently, the dissolution rate of element i was determined as a function of reaction time by plotting the rate determined at each sampling continuously. Quantitative information from the reacted glass surface analyses, i.e., the glass dissolution depth from the original surface, can also complement the consistent determination of glass dissolution rate.

3. Results and discussion

3.1. *pH dependence of glass dissolution rate*

Figure 3 shows the test results on the normalized dissolution rate of Si at 25°C as a function reaction time for each pH. Since Si is the major glass matrix constituent as shown in Table 1, the dissolution rate of Si can be assumed to indicate the dissolution rate of glass matrix. The results indicated that the dissolution rate at pH 3 and pH 11 is one order of magnitude higher than that at neutral pH. For the test at any pH,

the dissolution rate decreased slightly with time at the initial test period of up to 20 h, and then the rate reached at each constant value. According to our previous study [7,8], the relatively higher dissolution rate at the initial test period is suggested to be caused by mainly the larger surface area of initial glass specimen originated from the surface roughness by polishing, and the roughness becomes smoothed as the glass dissolution progresses to provide a constant dissolution rate at the test period of beyond 20 h.

With respect to the chemical affinity of solution, the concentrations of Si in the output solutions were measured to be around 7×10^{-6} M (0.2 ppm) at pH 3, and much less than that value at other pH. Since these values of Si concentration are much smaller than those of both solubility of SiO_2(am) (around 2×10^{-3} M at pH lower than 9) and the saturated Si concentration for P0798 glass dissolution (around 10^{-3} M at pH 9) [12], any solution condition examined in the present tests can be evaluated to be far from the saturation. According to a chemical affinity model proposed for dissolution of borosilicate waste glasses, the dissolution rate is given by the following equation based on a first-order dissolution rate law of SiO_2 dissolution [13]:

$$R = r_0\left(1 - \frac{a_{\mathrm{Si}}}{a_{\mathrm{sat}}}\right) + r_{\mathrm{residual}} \qquad (2)$$

where R is the dissolution rate of glass matrix; r_0 is the initial dissolution rate of glass matrix or forward dissolution rate, which depends on pH and temperature; a_{Si} is the actual activity of orthosilicic acid in solution or solution concentration of Si; a_{sat} is the corresponding activity at saturation or saturated concentration; and r_{residual} is the residual dissolution rate at saturation, which is much smaller than r_0.

In this model, the initial dissolution rate of glass matrix, r_0, is an intrinsic parameter representing the dissolution rate when the glass dissolves in Si-free solution, and the dissolution rate decreases with the increase of a_{Si}. Assuming that the chemical affinity model is applicable to the present test results on glass dissolution, the dissolution rate of Si measured in the present tests, NR_{Si}, can be assumed to indicate the r_0 at any pH, since the measured value of a_{Si} is much smaller than that of a_{sat} at any pH and the r_{residual} is much smaller than the r_0.

Assuming that the constant dissolution rate of Si obtained at the test period of beyond 20 h indicates the r_0 for each pH, the r_0 at 25°C was plotted against pH as shown in **Figure 4**. The results indicated that the r_0 shows a "V-shaped" pH dependence with a minimum at around pH 6, which is almost consistent with the previous results measured by using several different methods for several different waste glasses [4,14–17]. In order to confirm whether the present results on the r_0 shows a complete "V-shaped" pH dependence or not, a few additional data at around pH 6 are required to be obtained.

The test results on the normalized dissolution rates of B and Cs at 25°C as well as Si are shown in **Figure 5** as a function of reaction time for each pH. The results indicated that B and Cs, defined as "soluble elements" here, show almost the same dissolution rate each other at any pH. At pH 4 and pH 5.6 the dissolution rate of soluble elements was much higher than that of Si, and it decreased continuously with reaction time, which suggests that the soluble elements dissolve faster than silica glass matrix being controlled by a diffusion process to form a surface layer in which soluble elements are depleted. At pH 10, on the other hand, the dissolution rate of soluble elements was almost same as

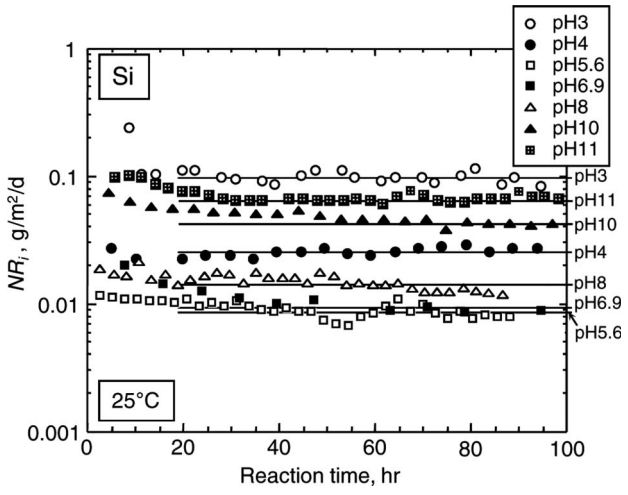

Figure 3. Normalized dissolution rate, NR_i, of Si at 25°C as a function of reaction time for each pH. Each horizontal line represents the average rate at the test period of beyond 20 h for each pH, which can be assumed to indicate initial dissolution rate, r_0.

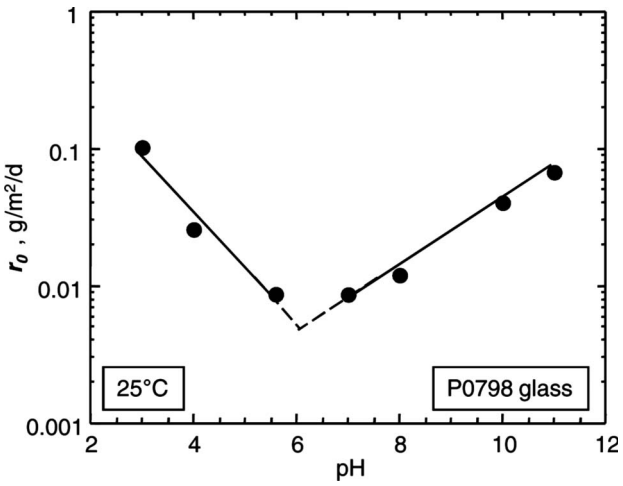

Figure 4. Initial dissolution rate, r_0, at 25°C as a function of pH.

that of Si, and it showed an almost constant value over the test duration, which suggests that the increase in pH accelerates the silica glass matrix dissolution and/or depresses the diffusion-controlled dissolution of soluble elements to result in the congruent dissolution. With respect to the diffusion-controlled dissolution of soluble elements, a mechanism based on diffusion of water or hydronium ion into the glass network by ion-exchange has been proposed for the glass dissolution under "saturation" conditions, and the diffusion coefficient has been evaluated to decrease with increase in pH for SON 68 and WAK glasses [18,19]. The present results on pH dependence of the dissolution of soluble elements under "far from saturation" conditions are also consistent with that of the diffusion evaluated under "saturation" conditions. Although the congruent dissolution has been assumed to be a dominant mechanism under "far from saturation" conditions in the previous models, e.g., the chemical affinity model described above, the present results suggest that the diffusion of water or hydronium ion resulting in the incongruent dissolution may play a certain role in the glass dissolution even under "far from saturation" conditions at acidic to neutral pH.

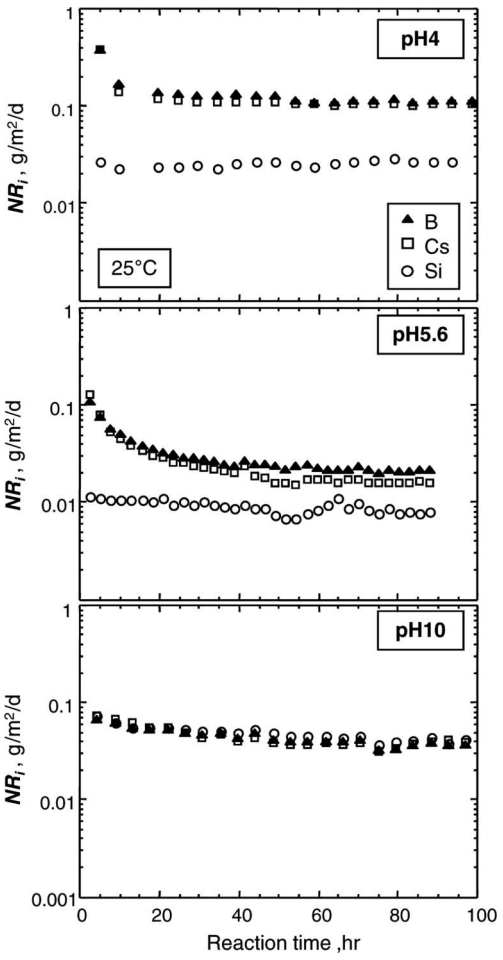

Figure 5. Normalized dissolution rate, NR_i, of B and Cs as well as Si at 25°C as a function reaction time for each pH.

3.2. *Temperature dependence of glass dissolution rate*

Figure 6 shows the test results on the normalized dissolution rate of Si at pH 5.6 as a function of reaction time for each temperature. With respect to the chemical affinity of solution, the concentration of Si in the output solution was measured to be much less than both solubility of SiO_2(am) and the Si saturated concentration for P0798 glass dissolution at any temperature. Assuming that the constant dissolution rate obtained at the test period of beyond 20 h indicates the r_0 for each temperature, Arrhenius plot of the r_0 is shown in **Figure 7**, where almost linear relation can be observed to give the apparent activation energy of 63 kJ/mol. This value of the activation energy is similar to that of 60 kJ/mol given by Delage for the initial dissolution rate of SON68 glass measured by using Soxhlet test method [20].

3.3. *Comparison between solution data and reacted glass surface data*

In order to confirm consistency of the present data on the glass dissolution rate determined from the solution analysis as described above, the reacted glass surface was analyzed to compare with the solution analysis data. After the dissolution test, some of the reacted glass specimens removed from the micro-channel reactor were dried at room temperature for a few days to be subjected to direct measurement of the dissolution depth from the initial surface using a surface roughness analyzer (Dektak 3). Since the glass surface subjected to the dissolution depth measurement was not pretreated except for drying, a certain

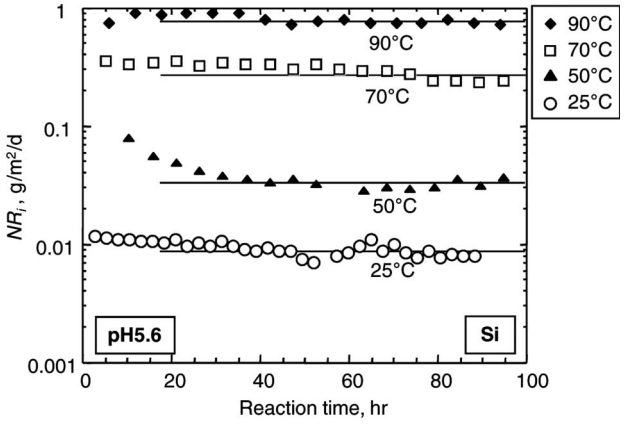

Figure 6. Normalized dissolution rate, NR_i, of Si at pH 5.6 as a function of reaction time for each temperature. Each horizontal line represents the average rate at the test period of beyond 20 h for each temperature, which can be assumed to indicate initial dissolution rate, r_0.

alteration layer may exist at the glass surface depending on the dissolution test condition.

Figure 8 shows the dissolution depth profile of the glass surface reacted at pH 10 with the reaction time of 171–213 h for each temperature, where the dissolution depth was measured along the solution flow from inlet to outlet at the center of reacted area marked by a horizontal broken line. Unfortunately, the dissolution depth was too shallow to be detected for the test at 25°C. In the present case of dissolution at pH 10, the solution analysis data shown in Figure 5 suggest that the glass dissolves congruently and the formation of surface alteration layer is expected to be unlikely. Then, on the assumption that the dissolved glass volume has an ideal rectangle cross section at any position along the solution flow, normalized elemental mass loss of Si, $NL(Si)$, was evaluated by using the average value of dissolution depth. Then, the average normalized dissolution rate throughout the test duration, $NR(Si)_{ave}$, was also evaluated by dividing the $NL(Si)$ by total reaction time, where the $NR(Si)_{ave}$ is not the same as the r_0, because the $NR(Si)_{ave}$ includes the relatively higher dissolution rate observed at the initial test period as shown in Figures 3, 5 and 6. On the other hand, the $NL(Si)$ and $NR(Si)_{ave}$ were also evaluated from the solution data by accumulating the amount of Si in each output solution to compare with that evaluated from the dissolution depth data. The results of comparison are summarized in **Table 3**(1). The values of $NL(Si)$ and $NR(Si)_{ave}$ evaluated from the dissolution depth data were almost consistent with that evaluated from the solution data at any temperature, which partly supports consistency of the present data on the glass dissolution rate. In the case of 50°C, however, values of $NL(Si)$ and $NR(Si)_{ave}$ evaluated from the dissolution depth data were relatively smaller than those from the solution data, in which disagreement can be considered to result from an error in the measurement of shallow dissolution depth of less than 1 μm.

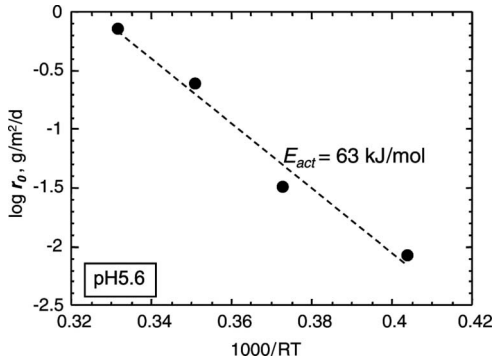

Figure 7. Arrhenius plot of the initial dissolution rate, r_0, at pH 5.6.

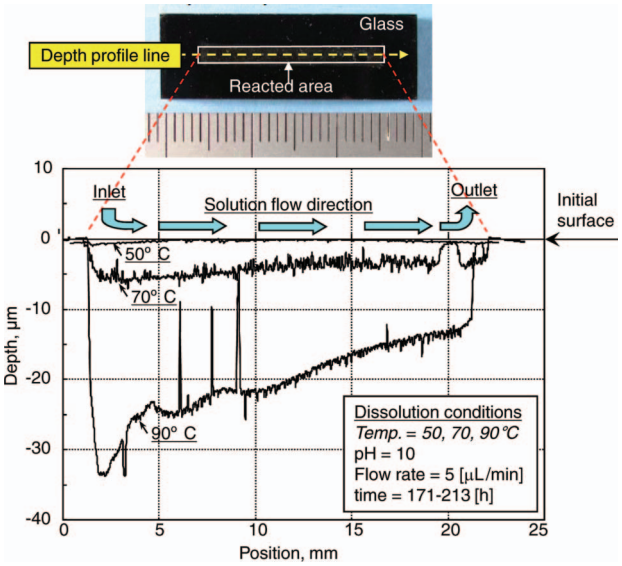

Figure 8. Dissolution depth profile of the reacted glass surface for each temperature obtained under test conditions of pH 10, solution flow rate of 5 μl/min, and reaction time of 171–213 h. Three large spikes observed in the depth profile for 90°C are assignable to insoluble particles (such as RuO_2) remaining on the reacted surface.

The dissolution depth profile shown in Figure 8 also gives another important information on the consistency of the present data, i.e., uniformity of the glass dissolution along the solution flow in the micro-channel. As shown in Figure 8 the depth profiles at 50 and 70°C were almost flat and parallel to the initial surface, which indicates that the glass dissolved uniformly along the solution flow in the micro-channel. The depth profile at 90°C, however, showed a steep slope along the solution flow where the dissolution depth near the inlet was larger than that near the outlet by a factor of 2, which indicates that the dissolution rate decreased along the solution flow in the micro-channel. **Figure 9** shows the dissolution depth profile of the glass reacted at 90°C for each pH, where the depth profile with a steep slope was observed at pH 3 as well as at pH 10, though the depth profile at pH 7 was almost flat and parallel to the initial surface. While the values of $NL(Si)$ and $NR(Si)_{ave}$ evaluated from the dissolution depth data were also consistent with those evaluated from the solution data at any pH as shown in Table 3(2). These results indicate that the decrease in glass dissolution rate along the solution flow occurs when the glass dissolution rate is high, i.e., at high temperature, basic pH, and acidic pH.

There are some potential mechanisms to account for the decrease in glass dissolution rate along the solution flow when the glass dissolution rate is high. The high glass dissolution rate can cause a change in the micro-channel dimensions leading to a change in the solution flow regime as a consequence of the progress in glass dissolution. However, the effect of the micro-channel dimension change can be assumed to be negligible, since the change

Table 3. Quantitative comparison between solution analysis data and reacted glass surface analysis data: Normalized elemental mass loss of Si, $NL(Si)$, and average normalized dissolution rate of Si, $NR(Si)_{ave}$, determined from solution data and from dissolution depth data.

Temp.	pH	Solution flow rate	Reaction time	$NL(Si)$ (g/m^2)		$NL(Si)_{ave}$ (g/m^2/day)	
				Solution data	Depth data	Solution data	Depth data
(1) Temperature dependence							
50°C	10	5 μl/min	213 h	2.26	1.15	0.25	0.13
70°C	10	5 μl/min	188 h	13.3	12.8	1.70	1.63
90°C	10	5 μl/min	171 h	47.2	58.8	6.62	8.25
(2) pH dependence							
90°C	*3*	5 μl/min	145 h	12.9	18.9	2.14	3.18
90°C	*7*	5 μl/min	270 h	7.28	7.79	0.65	0.69
90°C	*10*	5 μl/min	171 h	47.2	58.8	6.62	8.25
(3) Solution flow rate dependence							
90°C	3	*5* μl/min	145 h	12.9	18.9	2.14	3.18
90°C	3	*20* μl/min	120 h	24.2	24.5	4.84	4.90
90°C	10	*5* μl/min	171 h	47.2	58.8	6.62	8.25
90°C	10	*20* μl/min	182 h	75.6	72.9	9.97	9.61

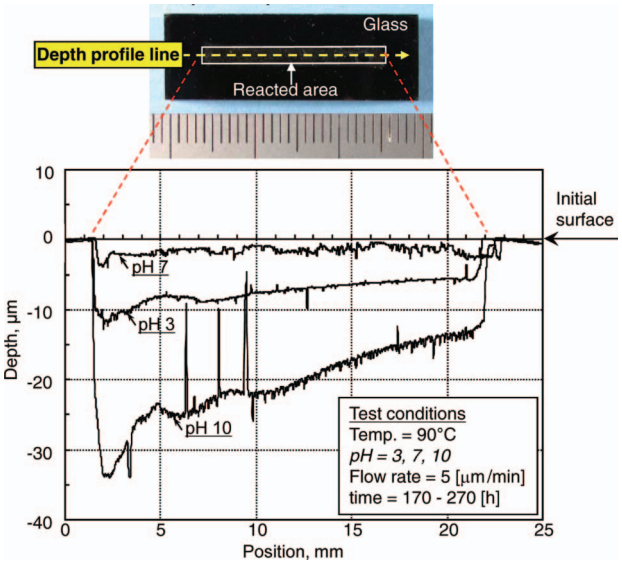

Figure 9. Dissolution depth profile of the reacted glass surface for each pH obtained under test conditions of 90°C, solution flow rate of 5 μl/min, and reaction time of 145–270 h.

in micro-channel dimensions, e.g., 30 μm deeper at maximum than the original depth of 0.16 mm in this case as shown in Figure 8, is too small to cause a certain change in the solution flow regime of completely laminar flow. The high glass dissolution rate can also cause a change in the solution chemical properties along the solution flow as a consequence of the progress in glass dissolution. The increase in solution concentration of Si along the solution flow can be proposed as one of the potential mechanisms accounting for the decrease in glass dissolution rate, because it can cause a decrease in the glass dissolution rate according to the first-order dissolution rate law described in Equation (2). However, the concentration of Si in output solution was measured to be less than the solubility of SiO_2(am) by a factor of more than 10 in any test case, which indicates that the effect of increase in solution concentration of Si is too small to account for the significant decrease in the glass dissolution rate observed in the present cases. The change in solution pH along the solution flow can also be proposed as another potential mechanism, because the glass dissolution rate changes sensitively with pH at both basic and acidic pH regions as shown in Figure 4, where a decrease in pH from 10 to 9.5 by 0.5 pH unit, for example, causes a decrease in the glass dissolution rate by a factor of more than 2. In the case of dissolution test at pH 10 and 90°C the concentration of Si in the output solution was measured to be around 2×10^{-4} M, which indicates that dissociation of the dissolved H_4SiO_4(aq) can occur to supply 2×10^{-4} M of H^+ into the solution at maximum according to the thermodynamic equilibrium calculation [11]. Although the solution pH is buffered partly by other glass–water related reactions, the increase in solution concentration of Si is expected to cause a certain decrease in solution pH. Therefore, the high glass dissolution rate at high temperature, basic pH, and acidic pH can be assumed to cause a certain change in the solution pH along the solution flow in the micro-channel to result in a significant decrease in the glass dissolution rate as the following manner,

At basic pH:

glass dissolution → increase in concentration of H_4SiO_4(aq) in solution → dissociation of H_4SiO_4(aq) into $H_3SiO_4^-$ supplying H^+ → decrease in pH → decrease in glass dissolution rate along the solution flow.

At acidic pH:

glass dissolution → increase in concentration of alkali metal elements in solution → increase in pH → decrease in glass dissolution rate along the solution flow.

If the change in solution pH is a dominant mechanism for the decrease in glass dissolution rate,

the glass dissolution tests with a higher solution flow rate are proposed to be an effective method to depress the pH change leading to the decrease in glass dissolution rate along the solution flow, though our previous studies confirmed that the glass dissolution rate is independent of the solution flow rate in the range from 2 μl/min to 20 μl/min when the glass dissolution rate is low at 25°C [7,8]. Therefore, additional dissolution tests with a higher solution flow rate of 20 μl/min, instead of the normal flow rate of 5 μl/min, were performed at 90°C for both pH 10 and pH 3. **Figure 10** shows the test results on dissolution depth profile of the glass surface reacted at pH 10 with the solution flow rate of 20 μl/min as well as 5 μl/min. The results indicated that the higher solution flow rate of 20 μl/min is effective for providing uniform glass dissolution with a flat dissolution depth profile parallel to the initial glass surface. The values of $NL(Si)$ and $NR(Si)_{ave}$ evaluated from both the solution data and the dissolution depth data in this case are also summarized in Table 3(3), which indicates that the higher solution flow rate gives the larger values of $NL(Si)$ and $NR(Si)_{ave}$ at both pH 10 and pH 3 as a result of the uniform glass dissolution. These results suggest that the solution flow rate is a key test condition to be accounted for precise and consistent measurement of the dissolution rate; that is, the higher solution flow rate is required for the measurement of the higher glass dissolution rate. On the other hand, too much higher solution flow rate causes a dilution of output solution preventing precise solution analysis. Therefore, an adequate flow rate is required to be adapted depending on each test condition. The present results on the dissolution depth profile indicate that the higher solution flow rate of 20 μl/min gives more precise and consistent data on the glass dissolution rate in the tests at 90°C for both pH 3 and pH 10.

3.4. *Initial dissolution rate as a function of pH and temperature*

The initial dissolution rate, r_0, was evaluated at each pH and temperature in the above way, and the results are summarized systematically as a function of pH and temperature in **Figure 11**, where the data at 90°C for both pH 3 and pH 10 were obtained by the tests with the higher solution flow rate of 20 μl/min according to the above discussion on the adequate solution flow rate. The results indicated that the r_0 increases with temperature at any pH, and the shape of pH dependence changes with temperature from "V-shaped" to "U-shaped." The r_0 shows a "V-shaped" pH dependence at 25°C, and it shows a "V-shaped" or "U-shaped" pH dependence at 50°C. Then, at 70°C and 90°C, it shows a completely "U-shaped" pH dependence with a flat bottom at neutral pH from 4 to 8. In Figure 11 the previous results on the r_0 measured by using SPFT method for 50°C and 90°C are also plotted as light broken lines for comparison [17]. At 50°C, the present MCFT results of "V-shaped" or "U-shaped" pH dependence are not so far from the SPFT results, though the MCFT results show slightly higher values of the r_0 at basic pH from 8 to 11. At 90°C, on the other hand, significant differences can be observed between the MCFT results and the SPFT results; that is, the MCFT results show a "U-shaped" pH dependence though the SPFT results show a "V-shaped" one, and the MCFT results also show certainly higher values of the r_0 at basic pH from 8 to 10 with a steeper slope. Some potential reasons can be proposed for interpreting the difference in the

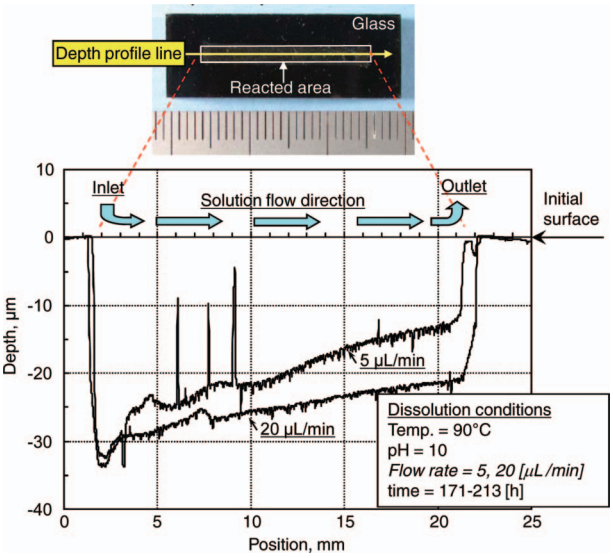

Figure 10. Dissolution depth profile of the reacted glass surface for each solution flow rate, obtained under test conditions of 90°C, pH 10, and reaction time of 171–182 h.

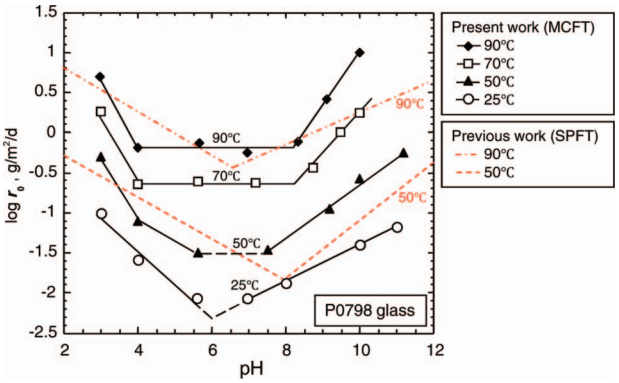

Figure 11. Initial dissolution rate, r_0, as a function of pH and temperature measured by using MCFT method for P0798 glass in comparison with that measured by using SPFT method [17]. The MCFT data at 90°C for both pH 3 and pH 10 were obtained under test conditions of higher solution flow rate of 20 μl/min, and other MCFT data were obtained under test conditions of normal solution flow rate of 5 μl/min.

results at 90°C between the two methods, and the most likely one is an error in determination of the glass surface area for the SPFT test. In the SPFT test using powdered glass specimen, the glass surface area decreases as the glass dissolution proceeds, which can lead to an underestimation of the glass dissolution rate. If the glass dissolution rate is low at low temperature and neutral pH, the decrease in glass surface area is small and the effects on the glass dissolution rate can be negligible. If the glass dissolution rate is high at higher temperature and acidic or basic pH, however, the decrease in glass surface area is estimated to be large enough to cause a certain underestimation of the glass dissolution rate, and a correction is required for the error in determination of glass surface area. For the SPFT results shown in Figure 11, however, details of the correction for error in glass surface area cannot be found in [17], and the further quantitative evaluation is difficult, unfortunately.

The "V-shaped" or "U-shaped" pH dependence of dissolution rate has been also observed in the hydrolysis of some minerals [21], and it can be related to changes in surface charge with pH where the shape of pH dependence of dissolution rate is usually symmetrical with respect to a neutral pH. However, the present results on the dissolution rate of waste glass indicated that the shape of pH dependence is not symmetrical with respect to a neutral pH at any temperature, which suggests that other additional processes than changes in surface charge with pH also affect the dissolution mechanism for the waste glass. In order to evaluate the mechanism in detail, much more data on the r_0, e.g., data at every 0.2 pH unit and at every 10°C, are required to be obtained for the future work.

From the present test results on temperature dependence of the r_0 shown in Figure 11, the apparent activation energy of the initial dissolution was evaluated for each pH. The results of Arrhenius plot of the r_0 are shown in **Figure 12** for pH 3, 5.6, and 10, where almost linear relation can be observed for each pH to give the apparent activation energy, E_{act}, from 54 kJ/mol at pH 3 to 76 kJ/mol at pH 10. **Figure 13** shows the E_{act} plotted against pH, where the E_{act} for pH 3, 4, 5.6 and 10 were determined from the data of r_0 measured directly at each pH and temperature, and the E_{act} for pH 5, 7, 8 and 9 were determined from the data of r_0 estimated by interpolation of the linear pH dependence at each temperature as shown in Figure 11. The results shown in Figure 13 indicate that the E_{act} increases with pH, which suggests that the dissolution mechanism can change depending on pH. At neutral pH from pH 5 to 9, the value of E_{act} is 60–70 kJ/mol, the value which is consistent with a surface-reaction-controlled-dissolution mechanism proposed for dissolution of borosilicate glass and SiO_2 polymorphs [20,22–24]. At acidic pH from pH 3 to 5, the value of E_{act} is around 50 kJ/mol, the value which is smaller than that for a surface-reaction-controlled-dissolution mechanism, but close to that for a diffusion-controlled-dissolution mechanism proposed for the residual dissolution of some waste glasses [25,26] and for diffusion of water or hydronium ion with ion-exchange in sodium alumino-silicate glasses [27]. The results suggest that the glass matrix dissolution under acidic pH conditions may be partly controlled by the diffusion process. At basic pH of pH 10, the value of E_{act} is 76 kJ/mol, the value which is slightly larger than that at neutral pH, suggesting that another different process may affect the glass matrix dissolution.

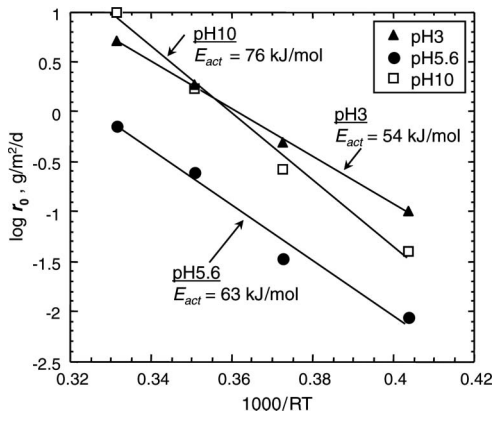

Figure 12. Arrhenius plot of the initial dissolution rate, r_0, measured by using MCFT method at pH 3, 5.6, and 10.

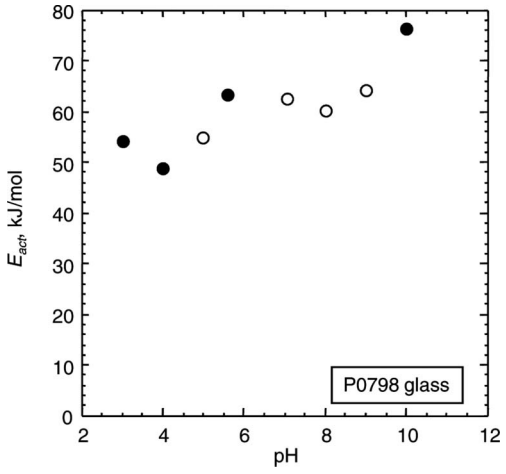

Figure 13. Apparent activation energy for initial dissolution of P0798 glass as a function of pH evaluated from temperature dependence of the r_0 measured by using MCFT method, where the data for pH 3, 4, 5.6, and 10 represented by solid circles were determined from the values of r_0 measured directly at each pH and temperature, and the data for pH 5, 7, 8 and 9 represented by open circles were determined from the values of r_0 estimated by interpolation of the linear pH dependence at each temperature as shown in Figure 11.

4. Conclusions

Aqueous dissolution tests were performed for a Japanese type of simulated HLW glass P0798 by using a newly developed MCFT test method to evaluate the initial dissolution rate of glass matrix, r_0, precisely and consistently as a function of solution pH (3–11) and temperature (25–90°C). The test results indicated that the r_0 shows a "V-shaped" pH dependence at 25°C, which is almost consistent with the previous results measured by using other test methods including SPFT method. At elevated temperatures of up to 90°C, however, the r_0 shows a "U-shaped" pH dependence with a flat bottom at neutral pH, which differs from the previous results measured by using SPFT method. The comparison with the SPFT results also indicated that the present MCFT results at 90°C show a certainly higher value of the r_0 with a steep slope of pH dependence than the SPFT results at basic pH from 8 to 11. With respect to the temperature dependence, the r_0 increases with the temperature according to an Arrhenius law at any pH, and the apparent activation energy evaluated from Arrhenius relation increases with pH from 54 kJ/mol at pH 3 to 76 kJ/mol at pH 10, which suggests that the dissolution mechanism can change depending on pH.

Acknowledgments

This work was partly supported by the JAEA Cooperative Research Scheme on the Nuclear Fuel Cycle. The authors wish to thank Dr. M. Watanabe from the Center of Advanced Instrumental Analysis, Kyushu University, for her help of the solution analysis using ICP-MS.

References

[1] Material Characterization Center (MCC), *Nuclear Waste Materials Handbook*, DOE/TIC 11400, Pacific Northwest Laboratory, USA, 1981.

[2] JK. Bates and M.J. Steindler, Alteration of nuclear waste glass by hydration, in *Scientific Basis for Nuclear Waste Management IV*, D.G. Brookins, ed., Mat. Res. Soc. Symp. Proc., Vol. 15, 1983, pp. 83–90.

[3] B.P. McGrail and D.K. Peeler, *Evaluation of the Single-pass flow-through Test to Support a Low-activity Waste Specification*, PNL-10746, Pacific Northwest Laboratory, USA, 1995.

[4] B.P. McGrail, W.L. Ebert, A.J. Bakel, and D.K. Peeler, Measurement of kinetic rate law parameters on a Na-Ca-Al borosilicate glass for low-activity waste, *J. Nucl. Mater.* 249 (1997), pp. 175–189.

[5] P.K. Abraitis, B.P. McGrail, D.P. Trivedi, F.R. Lives, and D.J. Vaughan, Single-pass flow-through experiments on a simulated waste glass in alkaline media at 40°C. I. Experiments conducted at variable solution flow rate to glass surface area ratio, *J. Nucl. Mater.* 280 (2000), pp. 196–205.

[6] *JSS Project Phase V Final Report, Testing and Modeling of the Corrosion of Simulated Nuclear Waste Glass Powders in a Waste Package Environment*, Technical Report – JSS Project 88-02, SKB, Stockholm, Sweden, 1988.

[7] Y. Inagaki, S. Mitsui, H. Makigaki, K. Idemitsu, T. Arima, T. Banba, and K. Noshita, Measurement of HLW glass dissolution/alteration kinetics by using micro-reactor flow-through test method, in *Scientific Basis for Nuclear Waste Management XXXIII*, B.E. Burakov and A.S. Aloy, eds., Mat. Res. Soc, Symp. Proc., Vol. 1193, 2010, pp. 219–228.

[8] H. Makigaki, Y. Inagaki, K. Idemitsu, T. Arima, S. Mitsui, T. Banba, and K. Noshita, Measurement of initial dissolution rate of P0798 simulated HLW glass by using micro-reactor flow-through test method, in *Scientific Basis for Nuclear Waste Management XXXIII*, B.E. Burakov and A.S. Aloy, eds., Mat. Res. Soc. Symp. Proc., Vol. 1193, 2010, pp. 307–314.

[9] K. Okuyama, A. Sasahira, K. Noshita, T. Yoshida, K. Kato, S. Nagasaki, and T. Ohe, A fast and sensitive method for evaluating nuclide migration characteristics in rock medium by using micro-channel reactor concept, *Phys. Chem. Earth* 32 (2007), pp. 463–468.

[10] K. Okuyama, A. Sasahira, K. Noshita, and T. Ohe, Cesium sorption rate on non-crushed rock measured by a new apparatus based on a micro-channel-reactor concept, in *Scientific Basis for Nuclear Waste Management XXX*, D. Dunn, C. Poinssot, and B. Begg, eds., Mat. Res. Soc. Symp. Proc., Vol. 985, 2007, pp. 449–455.

[11] D.L. Parkhurst, *Water-Resources Investigations Report* 95-4227, US Geological Survey, 1995.

[12] Y. Inagaki, H. Furuya, K. Idemitsu, and S. Yonezawa, Corrosion behavior of a powdered simulated nuclear waste glass: a corrosion model including diffusion process, *J. Nucl. Mater.* 208 (1994), pp. 27–34.

[13] B. Grambow, A general rate equation for nuclear waste glass corrosion, in *Scientific Basis for Nuclear Waste Management VIII*, C.M. Jantzen, J.A. Stone, and R.C. Ewing, eds., Mat. Res. Soc. Symp. Proc., Vol. 44, 1985, pp. 15–27.

[14] P.K. Abratis, D.J. Vaughan, F.R. Livens, J. Monteith, D.P. Trivedi, and J.S. Small, Dissolution of a complex borosilicate glass at 60°C: the influence of pH and proton adsorption on the congruence of short-term leaching, in *Scientific Basis for Nuclear Waste Management XXI*, I.G. McKinley and C. McCombie, eds., Mat. Res. Soc. Symp. Proc., Vol. 506, 1998, pp. 47–54.

[15] K.G. Knauss, W.L. Boucier, K.D. McKeegan, C.I. Merzbacher, S.N. Nguyen, F.J. Ryerson, D.K. Smith, H.C. Weed, and L. Newton, Dissolution kinetics of a simple analogue nuclear waste glass as a function of pH, time and temperature, in *Scientific Basis for Nuclear Waste Management XIII*, V.M. Obversby and P.W. Brown, eds., Mat. Res. Soc. Symp. Proc., Vol. 176, 1990, pp. 371–382.

[16] T. Advocat, J.L. Crovisier, E. Vernaz, G. Ehret, and H. Charpentier, Hydrolysis of R7T7 nuclear waste glass in dilute media: mechanisms and rate as a function of pH, in *Scientific Basis for Nuclear Waste Management XIV*, T. Abrajano, Jr., L.H. Johnson, eds., Mat. Res. Soc. Symp. Proc., Vol. 212, 1991, pp. 57–64.

[17] D.M. Strachan, W.L. Bourcier, and B.P. McGrail, Toward a consistent model for glass dissolution, *Radioact. Waste Manag Environ. Restor.* 19 (1994), pp. 129–145.

[18] B. Grambow and R. Muller, First-order dissolution rate law and the role of surface layers in glass performance assessment, *J. Nucl. Mater.* 298 (2001), pp. 112–124.

[19] K. Ferrand, A. Abdelouas, A. Abdelouas, and B. Grambow, Water diffusion in the simulated French nuclear waste glass SON 68 contacting silica rich solutions: experimental and modeling, *J. Nucl. Mater.* 355 (2006), pp. 54–67.

[20] F. Delage and D.L. Dussossoy, R7T7 glass initial dissolution rate measurements using a high-temperature Soxhlet device, in *Scientific Basis for Nuclear Waste Management XIV*, T. Abrajano, Jr., L.H. Johnson, eds., Mat. Res. Soc. Symp. Proc., Vol. 212, 1991, pp. 41–48.
[21] A.E. Blum and A.C. Lasaga, The role of surface speciation in the dissolution of albite, *Geochim. Cosmochim. Acta* 55 (1991), pp. 2193–2201.
[22] G. Berger, E. Cadore, J. Schott, and P.M. Dove, Dissolution rate of quartz in lead and sodium electrolyte solutions between 25 and 300°C: Effect of the nature of surface complexes and reaction affinity, *Geochim. Cosmochim. Acta* 58 (1994), pp. 541–551.
[23] P.J.N. Renders, C.H. Gammons, and H.L. Barnes, Precipitation and dissolution rate constants for cristobalite from 150 tp 300°C, *Geochim. Cosmochim. Acta* 59 (1995), pp. 77–85.
[24] L.J. Criscenti, J.D. Kubicki, and S.L. Brantley, Silicate glass and mineral dissolution: calculated reaction paths and activation energies for hydrolysis of a Q3 Si by H3O+ using Ab Initio methods, *J. Phys. Chem.* A 110 (2006), pp. 198–206.
[25] S. Gin, N. Godon, I. Ribet, P. Jollivet, Y. Minet, P. Frugier, E. Vernaz, J.M. Cavedon, B. Bonin, and R.D. Quang, Long-term behavior of R7T7-type nuclear glass: Current state of knowledge and outlook, in *Scientific Basis for Nuclear Waste Management XXVIII*, J.M. Hancher, S. Stroes-Gascoyne, and L. Browning, eds., Mat. Res. Soc. Symp. Proc., Vol. 824, 2004, pp. 327–332.
[26] Y. Inagaki, T. Saruwatari, K. Idemitsu, T. Arima, A. Shinkai, H. Yoshikawa, and M. Yui, Temperature dependence of long-term alteration rate for aqueous alteration of P0798 simulated waste glass under smectite forming conditions, in *Scientific Basis for Nuclear Waste Management XXIX*, P. Van Iseghem, ed., Mat. Res. Soc. Symp. Proc., Vol. 932, 2006, pp. 321–328.
[27] B.P. McGrail, J.P. Icenhower, D.K. Shuh, P. Liu, J.G. Darab, D.R. Baer, S. Thevuthasen, V. Shutthanandan, M.H. Engelhard, C.H. Booth, and P. Nachimuthu, The structure of Na_2O-Al_2O_3-SiO_2 glass: impact on sodium ion exchange in H_2O and D_2O, *J. Non-Cryst. Solids* 296 (2001), pp. 10–26.